Inorganic Chemistry

ARTICLE

pubs.acs.org/IC

Zinc(II) Complexes with a Versatile Multitopic Tetrazolate-Based Ligand Showing Various Structures: Impact of Reaction Conditions on the Final Product Structures

Tong-Liang Hu, Ying Tao, Ze Chang, and Xian-He Bu*

Department of Chemistry and Tianjin Key Laboratory of Metal & Molecule-based Material Chemistry, Nankai University, Tianjin 300071, China

Supporting Information

ABSTRACT: Four new zinc(II) complexes based on the same ligand, $\{Zn(ptp)(H_2O)\}_2$ (**1**), $[Zn(ptp)(CH_3OH)]_n$ (**2**), $[Zn(ptp)]_n$ (**3**), and $\{[Zn_3(ptp)_3](DMF)_2(H_2O)\}_n$ (**4**) [H_2ptp = 2,3-bis(pyridine-2-yl)-5,6-di-1*H*-tetrazol-5-ylpyrazine], have been synthesized by solvothermal methods. All of the complexes have been structurally characterized by elemental analysis, IR, powder X-ray diffraction, and single-crystal X-ray diffraction. Structural analyses show that complex **1** possesses a centrosymmetrical neutral dinuclear structure and **2** has 1D right-handed helical chains, with the 2_1 axis expanding along the crystallographic *b* direction; **3** features a 2D chiral-layered structure with (6,3) net, and complex **4** displays a 3D porous framework with $(4,12^2)$ topology. The various architectures (0D, 1D, 2D, and 3D) of these four complexes indicated that reaction conditions (temperature and solvent) play an important role in the formation of such coordination structures; namely, various structures can be obtained from the same reactants by controlling and changing the reaction conditions in this system. The luminescent properties of all of the complexes and the corresponding ligand have been investigated in the solid state at room temperature. Moreover, adsorption properties (N_2, H_2, O_2, CO_2, and CH_4) of the **4a** (desolvated **4**) have been studied, and the results show that **4a** possesses a moderate capability of gas sorption for N_2, H_2, O_2, and CO_2 gases, with high selectivity ratios for O_2 over H_2 at 77 K and CO_2 over CH_4 at 273 K.

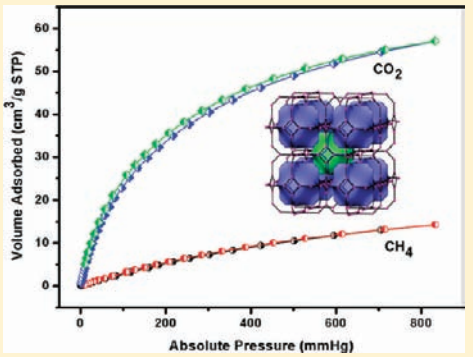

INTRODUCTION

The rational design and construction of metal−organic crystalline materials has been a hot topic for many years because of their enormous variety of structural topologies and potential applications as functional materials.[1] In recent years, porous metal−organic frameworks (PMOFs) have attracted increasing attention because they possess rich structural chemistry and excellent gas sorption properties. However, it is still difficult to explore feasible successful synthetic strategies for the preparation of PMOFs that have the desired structures and properties.[2] This results from the fact that many factors in the reaction process could affect the final structure of product, such as the reaction temperature,[3] solvent system,[4] pH value of the solution,[5] coordination geometry of the metal ions,[6] and auxilary ligands.[7] Hence, the controllable synthesis of stable PMOFs with high porosity becomes one of the most compelling challenges to chemists.

Recently, it was realized that multitopic tetrazolate-based organic ligands have great potential for fabricating PMOFs materials with novel network topologies and permanent porosity.[8,9] In our ongoing effort to construct PMOFs, we chose a multidentate ditopic tetrazolate-based ligand, 2,3-bis(pyridine-2-yl)-5,6-di-1*H*-tetrazol-5-ylpyrazine (H_2ptp), as the organic building block for the following purposes: (i) H_2ptp (or $Hptp^-$ and ptp^{2-} anions) has multiple coordination sites, and they may act as linkers to connect metal ions into higher dimensional structures through various coordination modes; (ii) H_2ptp has the features of rigidity and nonlinearity, which may reduce the probability of interpenetration; (iii) the nitrogen-rich backbone of H_2ptp may help in constructing supramolecular networks via hydrogen bonds and $\pi-\pi$ aromatic interactions; (iv) H_2ptp has the potential capability of constructing chiral MOFs owing to its coordination conformation.

In this study, we used the H_2ptp ligand and Zn^{II} ion as building blocks to construct complexes, aimed at obtaining useful MOF materials. Through control of the reaction conditions, a new series of complexes, $\{Zn(ptp)(H_2O)\}_2$ (**1**), $[Zn(ptp)(CH_3OH)]_n$ (**2**), $[Zn(ptp)]_n$ (**3**), and $\{[Zn_3(ptp)_3](DMF)_2(H_2O)\}_n$ (**4**; DMF = *N*,*N*-dimethylformamide), were obtained and structurally characterized. Taking the intense luminescent properties of d^{10} metal complexes into account, the luminescence properties of these complexes were also investigated in the solid state at room temperature. Furthermore, the gas adsorption properties (N_2, H_2, O_2, CO_2, and CH_4) of **4a** (desolvated complex **4**) have been

Received: July 19, 2011
Published: October 04, 2011

Table 1. Crystal Data and Structure Refinement Parameters for Complexes 1−4

	1	2	3	4
chemical formula	$C_{32}H_{20}N_{24}O_2Zn_2$	$C_{17}H_{12}N_{12}OZn$	$C_{16}H_8N_{12}Zn$	$C_{54}H_{40}N_{38}O_3Zn_3$
fw	903.46	465.76	433.71	1465.41
cryst syst	tetragonal	monoclinic	orthorhombic	triclinic
space group	$P4_2/n$	$P2_1$	$P2_12_12_1$	$P\bar{1}$
a/Å	20.961(3)	11.060(2)	8.0503(16)	13.551(3)
b/Å	20.961(3)	7.7694(16)	8.8185(18)	16.181(3)
c/Å	7.9322(16)	12.055(2)	22.972(5)	16.540(3)
α/deg	90	90	90	109.46(3)
β/deg	90	114.69(3)	90	101.21(3)
γ/deg	90	90	90	109.75(3)
V/Å^3	3485.1(10)	941.2(3)	1630.8(6)	3019.7(1)
Z	4	2	4	2
D/g cm^{-3}	1.722	1.643	1.767	1.612
T/K	293(2)	293(2)	293(2)	293(2)
μ/mm^{-1}	1.450	1.345	1.541	1.263
F(000)	1824	472	872	1487
R^a [$I > 2\sigma(I)$]	0.0602	0.0506	0.0301	0.0719
$R_w{}^b$ [all data]	0.0934	0.0807	0.0740	0.1445
Flack parameter		0.036(16)	0.003(15)	

$^a R = \Sigma||F_o| - |F_c||/\Sigma|F_o|$. $^b R_w = [\Sigma[w(F_o{}^2 - F_c{}^2)^2]/\Sigma w(F_o{}^2)^2]^{1/2}$.

studied. The results reveal that **4a** possesses moderate capability of gas sorption for N_2, H_2, O_2, and CO_2 gases, with high selectivity ratios for O_2 over H_2 at 77 K and CO_2 over CH_4 at 273 K.

EXPERIMENTAL SECTION

Materials and General Methods. All of the solvents and reagents for synthesis were obtained commercially and used as received. The ligand H_2ptp was synthesized by a modified literature method.[10] Elemental analyses (C, H, and N) were performed on a Perkin-Elemer 240C analyzer. The Fourier transform IR spectra were recorded from KBr pellets in the range 4000−400 cm^{-1} on a TENSOR 27 (Bruker) spectrometer. Powder X-ray diffraction (PXRD) was performed on a Rigaku D/Max-2500 diffractometer at 40 kV and 100 mA for a copper target tube and a graphite monochromator. Simulation of the PXRD spectra was carried out by the single-crystal data and diffraction-crystal module of the *Mercury* program available free of charge via the Internet at http://www.iucr.org. Emission spectra in the solid state at room temperature were taken on a Cary Eclipse fluorescence spectrophotometer. Thermogravimetric analyses (TGA) were performed on a Rigaku standard TG-DTA analyzer under an air atmosphere at a heating rate of 10 °C min^{-1} from ambient temperature to 800 °C for all measurements; an empty Al_2O_3 crucible was used as the reference.

Synthesis of Complexes. *{Zn(ptp)(H$_2$O)]$_2$* (***1***). A mixture of $Zn(NO_3)_2\cdot 6H_2O$ (120 mg, 0.4 mmol) and H_2ptp (74 mg, 0.2 mmol) with 12 mL of water and 1.5 mL of methanol was sealed in a 25 mL Teflon-lined stainless steel autoclave and heated to 180 °C. The autoclave was kept at 180 °C for 3 days and then cooled to room temperature. Orange block crystals were obtained, washed with water and methanol, and dried in air. Yield: ∼50% (based on H_2ptp). Anal. Calcd for $C_{32}H_{20}N_{24}O_2Zn_2$: C, 42.54; H, 2.23; N, 37.21. Found: C, 42.61; H, 2.49; N, 36.99. IR (KBr, cm^{-1}): 3125b, 1618w, 1562w, 1401s, 1187m, 1143w, 1120w, 1057w, 1035w, 1013w, 815m, 785w, 743w, 635w.

[Zn(ptp)(CH$_3$OH)]$_n$ (***2***). The method for the preparation of this complex was the same as that for **1**, wherein the autoclave was heated to 120 °C. Orange acetate crystals were isolated, washed with water and methanol, and dried in air. Yield: ∼30% (based on H_2ptp). Anal. Calcd $C_{17}H_{12}N_{12}OZn$: C, 43.84; H, 2.60; N, 36.09. Found: C, 43.53; H, 2.81; N, 36.29. IR (KBr, cm^{-1}): 3415b, 1618m, 1397s, 1182w, 1119w, 1089w, 1059w, 1033m, 789m, 763m, 744w, 636w, 565w, 535w.

[Zn(ptp)]$_n$ (***3***). The procedure for preparing complex **3** was the same as that for **1**, wherein the autoclave was heated to 170 °C. Orange prism-shaped crystals of **3** were isolated, washed with water and methanol, and dried in air. Yield: ∼20% (based on H_2ptp). Anal. Calcd $C_{16}H_8N_{12}Zn$: C, 44.31; H, 1.86; N, 38.75. Found: C, 44.52; H, 2.02; N, 38.46. IR (KBr, cm^{-1}): 1638m, 1618m, 1400s, 1118w, 789w, 621w, 478w.

{[Zn$_3$(ptp)$_3$](DMF)$_2$(H$_2$O)}$_n$ (***4***). A mixture of $Zn(NO_3)_2\cdot 6H_2O$ (120 mg, 0.4 mmol) and H_2ptp (74 mg, 0.2 mmol) with 6 mL of water and 7.5 mL of DMF was sealed in a 25 mL Teflon-lined stainless steel autoclave and heated to 100 °C. The autoclave was kept at 100 °C for 1 day and then cooled to room temperature. Orange block crystals were obtained, washed by water and ethanol, and dried in air. Yield: ∼40% (based on H_2ptp). Anal. Calcd for $C_{54}H_{40}N_{38}O_3Zn_3$: C, 44.26; H, 2.75; N, 36.32. Found: C, 44.57; H, 2.64; N, 36.42. IR (KBr, cm^{-1}): 1658m, 1472w, 1407s, 1247w, 1179m, 1094m, 1061w, 1012w, 790m, 754w, 636w, 540w.

X-ray Crystallography. Single-crystal X-ray diffraction data for complexes **1**−**4** were collected on a Rigaku SCX-mini diffractometer at 293(2) K with Mo Kα radiation (λ = 0.710 73 Å) in the ω-scan mode. The program *SAINT*[11a] was used for integration of the diffraction profiles. All of the structures were solved by direct methods using the *SHELXS* program of the *SHELXTL* package and refined by full-matrix least-squares methods with *SHELXL*.[11b] Semiempirical absorption corrections were carried out using the *SADABS* program.[11c] Zn atoms in the complexes were located from the *E* maps, and other non-H atoms were located in successive difference Fourier syntheses and refined with anisotropic thermal parameters on F^2. The H atoms of the ligand (H_2ptp) and organic solvents (DMF and CH_3OH) were generated theoretically onto the specific atoms and refined isotropically with fixed thermal factors. H atoms of water molecules were added by the difference Fourier maps. Crystal data and structure refinement parameter details for complexes **1**−**4** are given in Table 1, and the selected bond lengths and angles are given in Tables S1−S4 (Supporting Information).

dx.doi.org/10.1021/ic2015463 |*Inorg. Chem.* 2011, 50, 10994–11003

Sorption Measurements. Gas sorption experiments were carried out with a Micrometrics ASAP 2020 M volumetric gas sorption instrument. Before measurement, the sample was soaked in dichloromethane (CH_2Cl_2) for 3 days to remove DMF and then filtered and dried at room temperature. Then the sample was loaded into the sample tube and dried under a high vacuum (less than 10^{-5} Torr) at 85 °C overnight to remove CH_2Cl_2 and all residue solvents in the channels. About 80 mg of the desolvated sample was used in all of the adsorption measurements. The H_2 sorption isotherms were collected in a pressure range from 10^{-4} to 1 atm at 77 K in a liquid-N_2 bath and at 87 K in a liquid-Ar bath, respectively. The O_2 isotherm measurement was proceeded at 77 K. The gas sorption experiments of CO_2 and CH_4 were carried out at 273 K in an ice−water bath.

RESULTS AND DISCUSSION

Synthesis Consideration and General Characterization. Solvothermal synthesis has been widely used to prepare new materials with diverse structures, although the mechanism may be not completely clear.[12] This method may minimize the problems associated with ligand solubility and enhance the reactivity of the reactants. Because the structures of metal−organic crystalline materials can be affected by many factors in the reaction process, the controllable synthesis of MOFs with desired structures and properties becomes one of the most compelling challenges to chemists. In this work, four new complexes with various architectures (0D, 1D, 2D, and 3D) have been obtained from the same reactants by changing the reaction conditions (temperature or solvent). This should be a good example of how the reaction conditions impact the final product structure. It should be noted that the addition of methanol/DMF as the solvent is the key point for the synthesis process. The attempt to obtain the complex with pure water as the solvent was not successful as the ligand has limited solubility in water even at rather high temperature. On the other hand, the ligand is soluble in methanol and DMF, and then these solvents were added to increase the solubility of the ligand in the reaction systems.

Complexes **1**−**4** are all air-stable. All general characterizations were carried out with crystalline samples. Elemental analyses showed that the components of these complexes are well consistent with the results of structural analysis of **1**−**4**. The IR spectra of all four complexes show absorption bonds resulting from the skeletal vibrations of the aromatic rings in the 1397−1638 cm^{-1} range. In the IR spectra of **1**, the broad band centered at ∼3125 cm^{-1} indicates the O−H stretching of the aqua molecules. The spectra of **2** exhibit broad bands at ∼3415 cm^{-1} because of the O−H stretching of the methanol molecules. For **4**, the IR spectra display the characteristic bands of the carbonyl group of DMF at 1658 cm^{-1}.

Description of Crystal Structures. *Complex **1***. The structure of the centrosymmetrical neutral dinuclear complex **1** is shown in Figure 1a. Each Zn^{II} ion is 5-coordinated to four N atoms (two tetrazole N, one pyridine N, and one pyrazine N atoms) of two distinct ptp^{2-} [with Zn−N lengths being 2.009(3)−2.177(3) Å] and one O atom from the coordinated water molecule [Zn−O = 1.973(3) Å]. The selected bond distances and angles are listed in Table S1 (Supporting Information). In **1**, two ptp^{2-} ligands bridge two Zn^{II} atoms to form a binuclear structure containing a 12-membered ring, in which the Zn···Zn distance is 5.497 Å. Each ptp^{2-} ligand chelates one Zn^{II} center and simultaneously bridges the other one, showing a quadridentate chelating−bridging mode (mode I, Scheme 1). Moreover, neither the two tetrazolate rings nor the two pyridine rings in each ligand are parallel, and dihedral angles of 56.1° and 51.8° are formed, respectively. Also, different torsional degrees of each tetrazolate/pyridine ring with the pyrazine plane lead to dihedral angles of 14.0, 43.2, 17.6, and 35.4°, respectively.

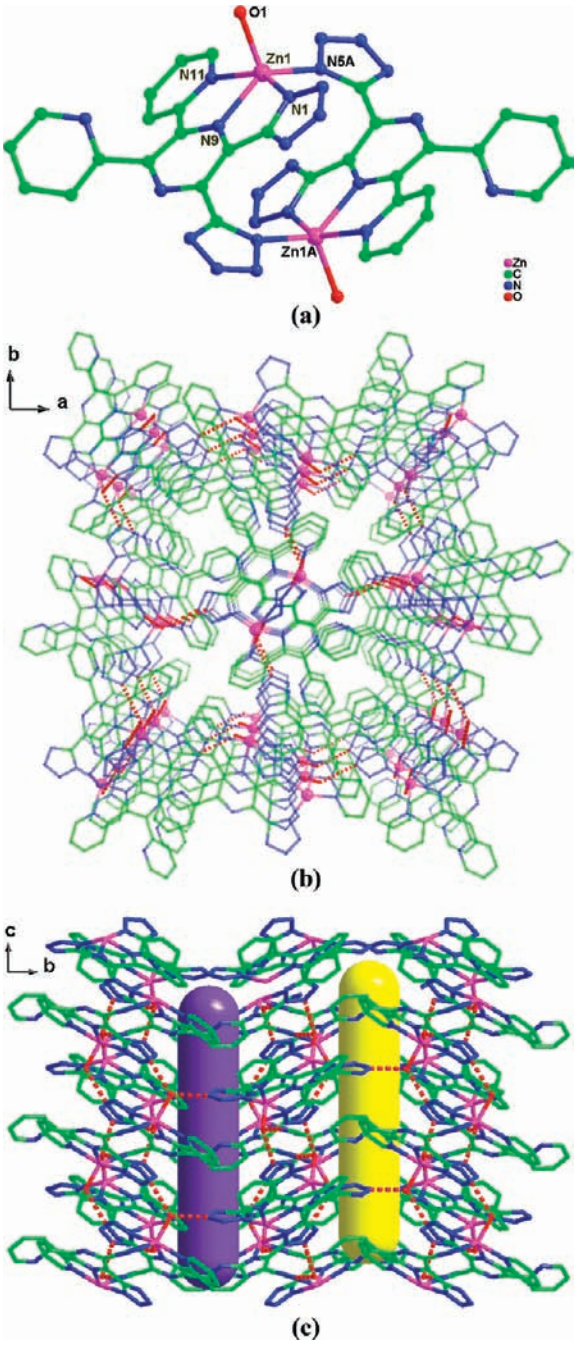

Figure 1. Crystal structure of **1**: (a) centrosymmetrical neutral dinuclear molecular structure; (b) 3D supramolecular framework constructed of strong intermolecular hydrogen bonds; (c) two kinds of 1D channels in the 3D supramolecular network.

In the crystal structure of **1**, as shown in Figure 1b, the neutral dinuclear molecules are bound together by strong intermolecular hydrogen bonds to create a 3D supramolecular network. The hydrogen-bonding system in **1** consists of the N atoms N3 and

dx.doi.org/10.1021/ic2015463 |*Inorg. Chem.* 2011, 50, 10994–11003

Scheme 1. Coordination Modes of ptp^{2-}

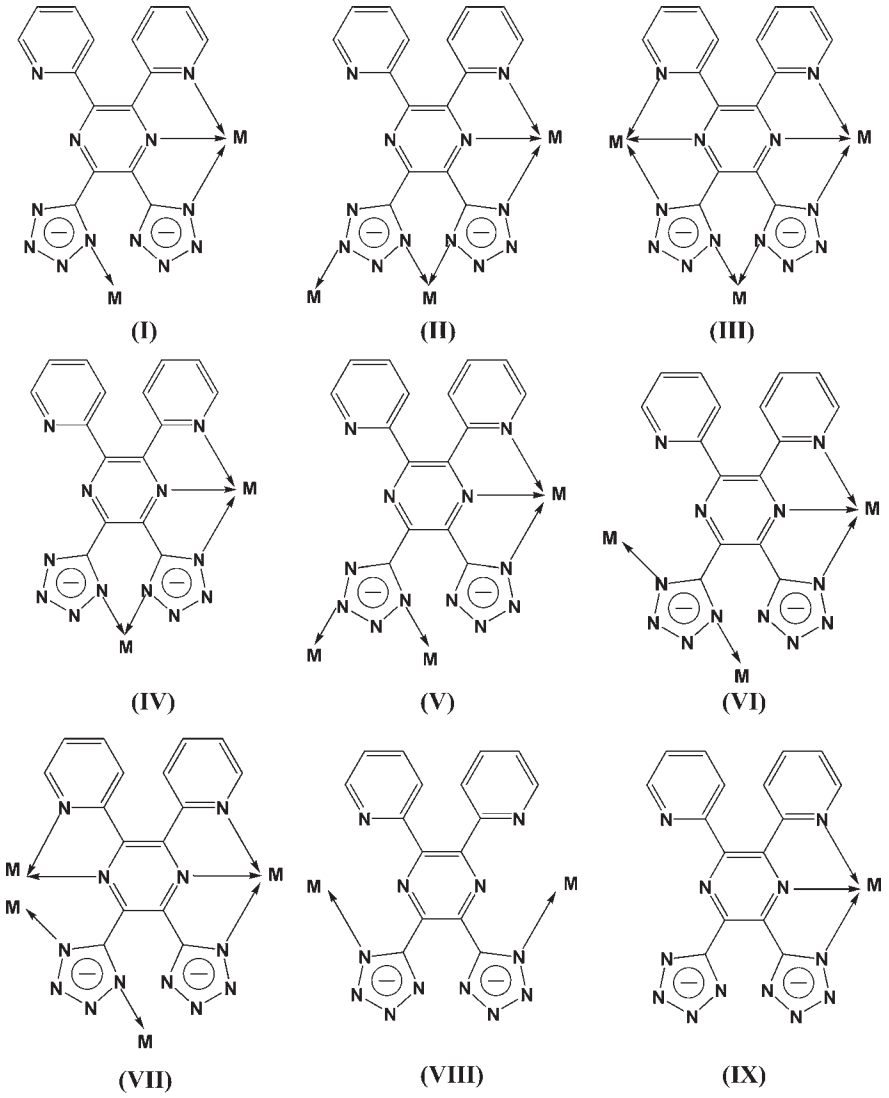

N7 on two tetrazolate rings, with the H atoms H1A and H1B on the coordinated water molecule O1 of neighboring molecules. The N3···H1A (N7···H1B) distance is 1.820(5) Å [1.869(6) Å], the corresponding N3···O1 (N7···O1) distance is 2.711(5) Å [2.703(5) Å], and the O1−H1A···N3 (O1−H1B···N7) angle is 173.8(3)° [167.7(5)°]. Each molecule was connected to six neighboring molecules through hydrogen bonds. There is no doubt that these strong hydrogen-bonding interactions contribute significantly to the alignment of the molecules of **1** in the crystalline state. In addition, two kinds of 1D channels are formed among the supramolecular network (Figure 1c).

Complex ***2***. Complex **2** crystallizes in the chiral space group $P2_1$. The asymmetric unit of **2** contains one Zn^{II}, one ptp^{2-} ligand, and one methanol molecule (Figure 2), in which Zn^{II} shows a disordered octahedral coordination geometry that is coordinated by one O atom from a methanol molecule and five N atoms (one pyridine N, one pyrazine N, and three tetrazolate N atoms) of two distinct ptp^{2-} ligands. The bond angles around Zn^{II} range from 73.96(2) to 175.03(2)°. The Zn−N [ranging from 2.031(4) to 2.215(4) Å] and Zn−O [2.115(4) Å] bond lengths in **2** are in the expected range for such complexes (bond distances for Zn−N and Zn−O and angle for N−Zn−O; see Table S2 in the Supporting Information).[8,13] In **2**, each ptp^{2-} ligand chelates one Zn^{II} center with three N atoms (one pyridine N, one pyrazine N, and one tetrazolate N atoms) and simultaneously chelates another Zn^{II} center by two tetrazolate N atoms, showing a quinquidentate chelating−chelating mode (mode IV, Scheme 1). Moreover, the two tetrazolate rings (or two pyridine rings) in each ligand are not parallel, and a dihedral angle of 54.4° (52.2°) is formed. Also, different torsional degrees of each tetrazolate/pyridine ring with the pyrazine plane lead to dihedral angles of 29.3, 38.9, 30.9, and 37.6°, respectively. The ptp^{2-} ligands in **2** alternately bridge the Zn^{II} atoms to form a 1D right-handed helical infinite chain of $[Zn(ptp)]_n$ around the crystallographic 2_1 axis expanding along the crystallographic *b* direction, in which the pitch is 7.769 Å and the Zn···Zn distance is 5.964 Å (Figure 2b).

In the crystal structure of **2**, as shown in Figure 2c, there exist strong intermolecular hydrogen bonds between the adjacent helical chains. The intermolecular O−H···N hydrogen-bonding interactions between the N atom from one tetrazolate ring and the OH group of a methanol molecule [the N7···H1A distance is 1.789(9) Å, the corresponding N7···O1A distance is

dx.doi.org/10.1021/ic2015463 |*Inorg. Chem.* 2011, 50, 10994–11003

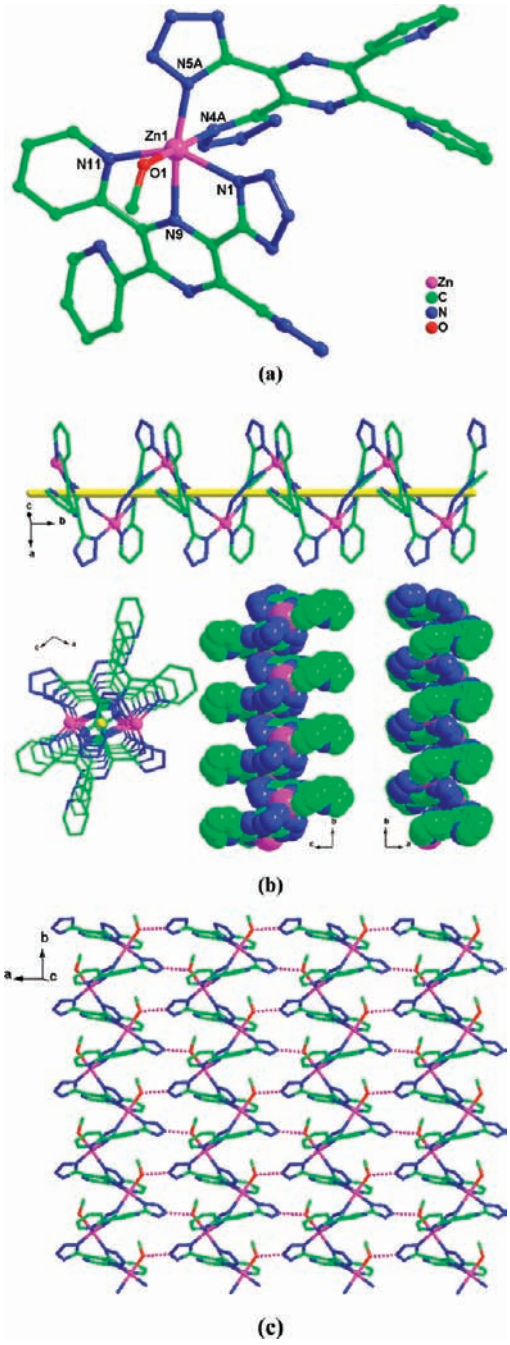

Figure 2. Crystal structure of **2**: (a) coordination geometry of Zn^{II}; (b) 1D helix structure along the *b* axis; (c) homochiral 2D sheet constructed by strong hydrogen bonds.

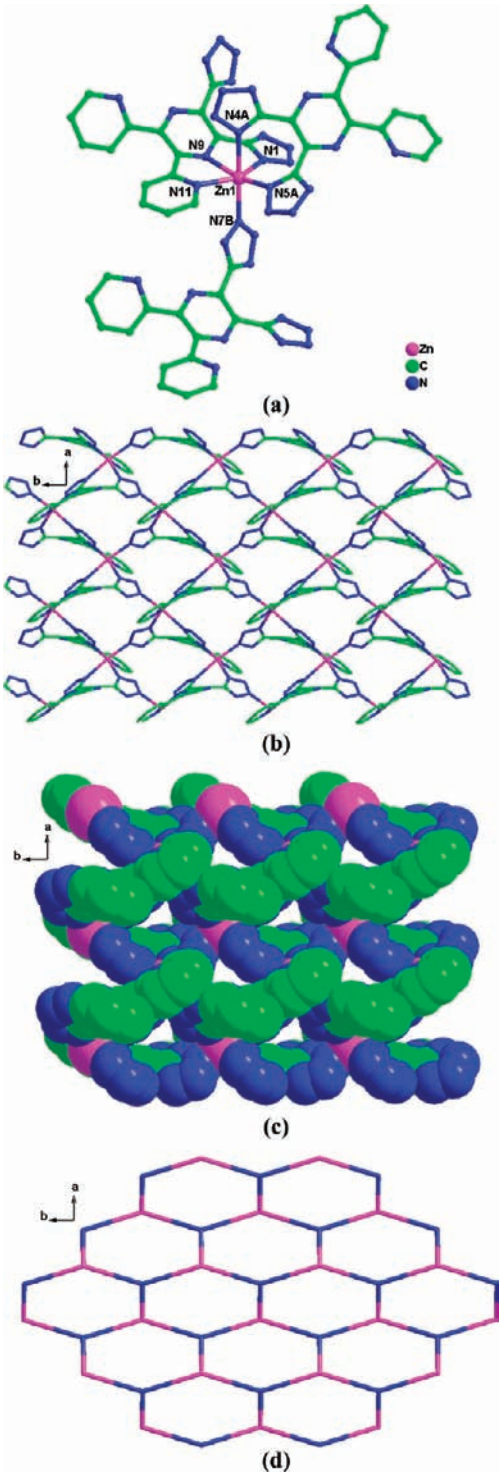

Figure 3. Crystal structure of **3**: (a) coordination geometry of Zn^{II}; (b) 2D layer structure; (c) space-filled representation of the 2D layer structure; (d) (6,3)-net topology with Zn^{II} and ptp^{2-} ions as three-connected nodes.

2.664(7) Å, and the O1A−H1A···N7 angle is 156.8(8)°] lead to the formation of a homochiral 2D sheet (Figure 2c), in which all of the helical chains are right-handed chirality. On the other hand, the polar and chiral space group $P2_1$ indicates a specific direction of polarization along the *b* axis. This should also be attributed to the AA style of stacking of the homochiral 2D layers. Such complexes with asymmetric or polar coordination geometries are likely to display NCS structures and exhibit good second harmonic generation properties.[14] Because self-assembly via intermolecular noncovalent interactions is one of the most powerful tools for designing and synthesizing polar crystals as well as enantioselective chiral host frameworks,[15] the complex reported here offers great potential for materials with interesting optoelectric properties and new functions.

Complex ***3***. Complex **3** crystallizes in the orthorhombic chiral space group $P2_12_12_1$ and exhibits a 2D (6,3) topological layer

dx.doi.org/10.1021/ic2015463 |*Inorg. Chem.* 2011, 50, 10994–11003

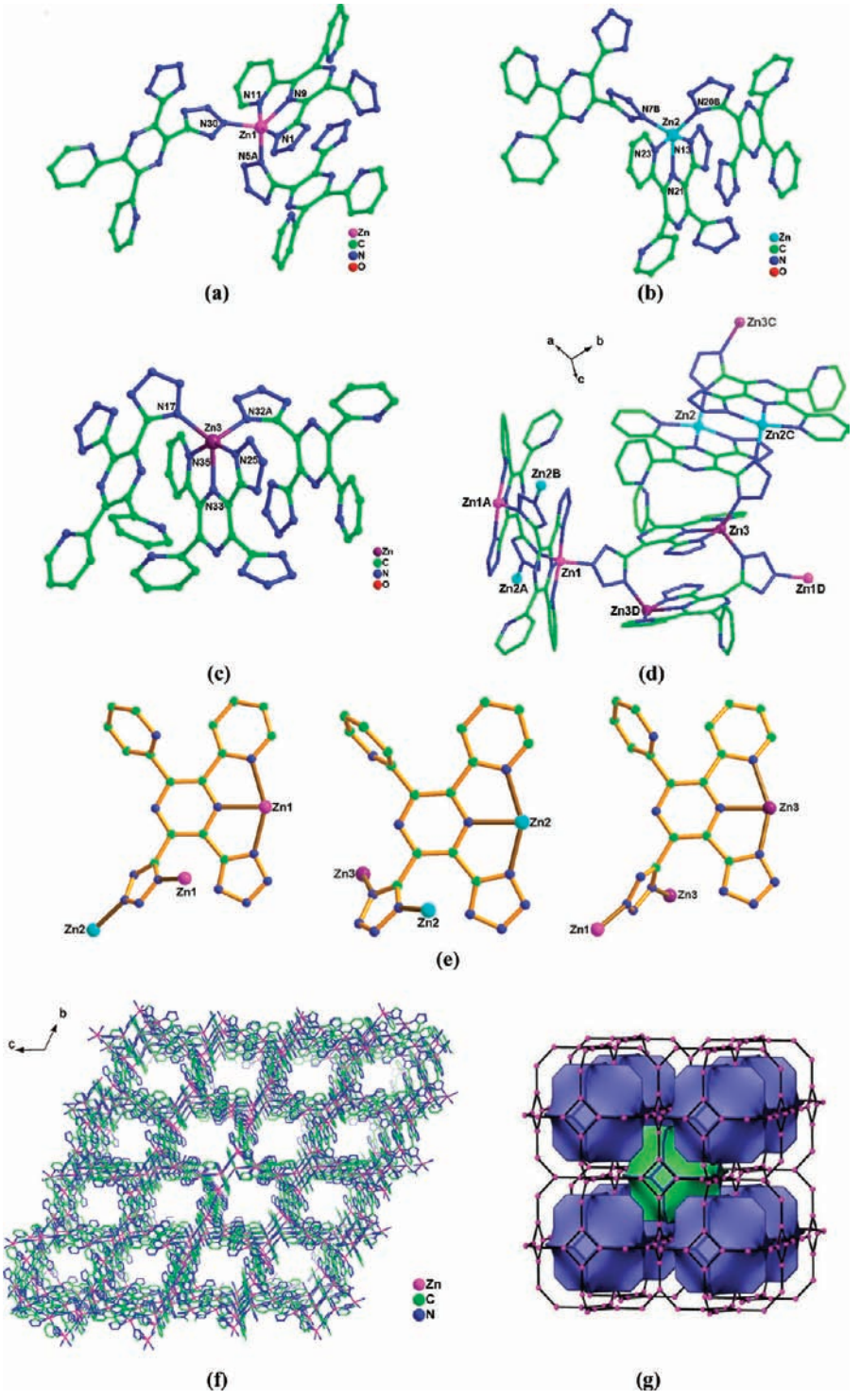

Figure 4. Crystal structure of **4**: (a) coordination geometry of Zn1; (b) coordination geometry of Zn2; (c) coordination geometry of Zn3; (d) connection mode of three kinds of Zn^{II} centers; (e) coordination modes of ligand ptp^{2-}; (f) 3D framework showing 1D open channels along the *a* axis (H atoms, uncoordinated pyridine rings, and solvent molecules are omitted for clarity); (g) tilling view of the $(4,12^2)$-net topology with Zn^{II} and ptp^{2-} ions as three-connected nodes.

structure. As shown in Figure 3a, the asymmetric unit of **3** is composed of a 6-coordinated zinc center and a ptp^{2-} ligand, in which the 6-coordinated Zn center is in a slightly distorted octahedral coordination environment that is coordinated by six N atoms (one pyridine N, one pyrazine N, and four tetrazolate N atoms) of three distinct ptp^{2-} ligands. The bond angles around Zn^{II} range from 72.60(1) to 173.32(1)°. The Zn−N [ranging from 2.074(3) to 2.319(3) Å] bond lengths in **3** are in the expected range for such complexes (bond distances for Zn−N and angles for N−Zn−N; see Table S3 in the Supporting Information).[8,13]

dx.doi.org/10.1021/ic2015463 |*Inorg. Chem.* 2011, 50, 10994–11003

In **3**, the ptp^{2-} ligand chelates two Zn^{II} centers with three N atoms (one pyridine N, one pyrazine N, and one tetrazolate N atoms) and two tetrazolate N atoms, respectively, and simultaneously bridges the other Zn^{II} center, showing a hexadentate chelating−chelating−bridging mode (mode II, Scheme 1). Moreover, the two tetrazolate rings (or two pyridine rings) in each ligand are not parallel, and a dihedral angle of 61.2° (54.7°) is formed. Also, different torsional degrees of each tetrazolate/pyridine ring with the pyrazine plane lead to dihedral angles of 26.5, 46.0, 26.6, and 36.4°, respectively. Each hexadentate bridging ligand is bound to three metal ions, and each metal ion is linked to four other metal ions by two ptp^{2-} ligands. These give rise to a 2D sheet parallel to the *ab* plane, with adjacent Zn···Zn separations of 6.267 and 6.202 Å, respectively (Figure 3b−d). The planes further generated a 3D network via one kind of $\pi\cdots\pi$-stacking interaction between the pyridine rings from two adjacent ptp^{2-} ligands with an interplanar separation of 3.112 Å (the centriod−centriod distance is 3.954 Å), belonging to medium-strength $\pi\cdots\pi$-stacking interactions.[16]

Complex ***4***. Complex **4** crystallizes in the triclinic space group $P\bar{1}$ and exhibits a 3D porous framewok with 1D open channels. As shown in Figure 4, there exist three symmetry-independent Zn^{II} ions (Zn1, Zn2, and Zn3) in the crystallographic asymmetric unit, which all adopt similar coordination geometries. Each Zn^{II} center is 5-coordinated to five N atoms (one pyridine N, one pyrazine N, and three tetrazolate N atoms) of three distinct ptp^{2-} ligands. The bond angles around Zn^{II} range from 73.57(2) to 149.66(2)° (for Zn1), from 73.89(2) to 149.45(2)° (for Zn2), and from 73.33(2) to 150.1(2)° (for Zn3). The Zn−N [ranging from 2.018(5) to 2.193(5) Å (for Zn1), from 2.013(5) to 2.169(5) Å (for Zn2), and from 2.018(5) to 2.217(5) Å (for Zn3)] bond lengths in **4** are in the expected range for such complexes (bond distances for Zn−N and angles for N−Zn−N; see Table S4 in the Supporting Information).[8,13] In the crystal structure of **4**, as shown in Figure 4e, ptp^{2-} ligand have three kinds of conformations, which are all showing a quinquidentate chelating−bridging−bridging mode (modes V and VI, Scheme 1). Moreover, there are different dihedral angles between the planes of aromatic heterocycles (tetrazolate, pyridine, and pyrazine rings; Table S5 in the Supporting Information). Each ptp^{2-} ligand chelates one Zn^{II} center with three N atoms (one pyridine N, one pyrazine N, and one tetrazolate N atoms), simultaneously bridging the other two Zn^{II} centers by two N atoms of one tetrazolate ring. Each quinquidentate bridging ligand is bound to three metal ions, and each metal ion is linked to four other metal ions by two ptp^{2-} ligands. These give rise to a 3D framework containing 1D open channels along the *a* axis. The channels are filled with guest DMF and water molecules. The free void volume of **4** estimated by *PLATON*[17] is 24.5% of the total volume when the guest molecules are removed. The simplification of the 3D framework of **4** by regarding each Zn^{II} atom and each ptp^{2-} ligand as three-connecting nodes resulted in a uniform $(4,12^2)$ net (Figure 4f).

Comparing the structures of complexes **1**−**4**, we found that the dimensionality of the resulting compounds was mainly determined by the conformations of ptp^{2-} as well as the connection mode between the metal centers and ligands. As shown in Table S5 (Supporting Information), there are different dihedral angles between the planes of aromatic heterocycles (tetrazolate, pyridine, and pyrazine rings) in every ptp^{2-}. However, the sums of all dihedral angles in one ptp^{2-} of complexes **1**−**4** are gradually increasing in the order of 0D, 1D, 2D, and 3D. The increased dihedral angles indicate the fact that the environments around the coordinated groups, especially for tetrazolate rings, become more crowded with an increase of the structure dimension. In complexes **1** and **2**, each Zn^{II} center connects with two ligands and each ligand bridges two Zn^{II} centers as well, while in complexes **3** and **4**, the coordination numbers both become 3. Then the increased connections resulted in more complicated structures. Furthermore, in the reported complexes, the connection mode between the ligand and Zn^{II} is determined by the conformation of the metal ions, which is directly affected by the solvent systems and reaction temperatures. When reactions are processed under 180 or 120 °C, one of the coordination sites of the 5- or 6-coordinated Zn^{II} centers is occupied by a solvent molecule, and relatively simple complexes **1** and **2** are obtained, respectively. In complexes **3** and **4**, all of the coordination sites of the metal centers are possessed by ptp^{2-} ligands, and then more complicated structures are produced. So, we can say that the changes of the reaction conditions affect the conformations of the ptp^{2-} ligand and metal centers, which finally determine the dimensionality of the target compounds.

PXRD and TGA. The phase purity of **1**−**4** was confirmed by PXRD analysis on bulk samples. The PXRD profile of each as-synthesized complex well matched the simulated ones based on the single-crystal X-ray structure (Figure S2 in the Supporting Information for **1**−**4**). Prior to gas sorption experiments, water and DMF molecules are removed from compound **4** by solvent exchanges. The solvent-exchanged sample was then dried under a high vacuum to obtain the desolvated solid **4a**. The activated sample **4a** is still crystalline, as evidenced by the PXRD patterns. Although the experimental patterns of the activated sample **4a** show a few unindexed peaks and slightly broadened diffraction lines that might be attributed to the slight change of the structure caused by removal of the guest molecules, the whole porous framework should remain. To examine the thermal stability of **4**, a TGA experiment was performed by heating the crystalline sample (Figure S1 in the Supporting Information). The TGA curve of **4** reveals that the first weight loss of 3% in the temperature region of 195−295 °C corresponds to the expulsion of lattice water and partial DMF molecules. The residual component starts to decompose beyond 300 °C with two step weight losses (peaking at 305 and 527 °C). TGA of **4** showed that it is stable to 300 °C (Figure S3 in the Supporting Information).

Adsorption Properties. Gas sorption experiments of the desolvated solid **4a** were carried out for N_2, O_2, H_2, CO_2, and CH_4 gases to investigate its pore structure and gas storage capability. The results of gas adsorptions of **4a** are listed in Table 2.

To investigate the porosity of **4a**, N_2 sorption was performed at 77 K. The uptake amount of N_2 is 93.96 cm^3/g (STP) at $P/P_0 = 1.0$, and the gas sorption shows a reversible type I isotherm with no hysteresis upon desorption (Figure 5a), being characteristic of microporous material. The Brunauer−Emmett−Teller and Langmuir surface areas of the guest-free framework were estimated to be 322.56 and 421.98 $m^2\ g^{-1}$, respectively, and the Horvath−Kawazoe (H−K)[18] pore diameter is 4.98 Å (Figure S4 in the Supporting Information). Furthermore, the H−K pore volume is 0.15 $cm^3\ g^{-1}$, a little lower than the value of 0.17 $cm^3\ g^{-1}$ calculated from the crystal structure, which indicates that the gas molecules fill the void space efficiently.

Table 2. Gas Adsorption Data for 4a

gas	temperature and pressure	amount of gas adsorbed		
		wt %	$cm^3\ g^{-1}$	mmol g^{-1}
N_2	77 K and P/P_0 = 1.0	11.74	93.96	4.19
O_2	77 K and P/P_0 = 0.9	20.38	142.32	6.37
H_2	77 K and 800 mmHg	0.84	94.27	4.21
	87 K and 800 mmHg	0.62	69.10	3.08
CO_2	273 K and 832 mmHg	11.21	57.08	2.55
CH_4	273 K and 833 mmHg	1.02	14.29	0.64

The accessible porosity in **4a** confirmed by the N_2 sorption study prompts us to further investigate the gas sorption properties of **4a**. Subsequently, O_2 and H_2 adsorption measurements were carried out. In the case of O_2 adsorption, **4a** adsorbs up to 20.38 wt % (142.32 $cm^3\ g^{-1}$, 6.37 mmol g^{-1}, STP) at 77 K and P/P_0 = 0.9 (Figure 5a).

The H_2 sorption isotherms at 77 and 87 K both show type I behavior with slight hysteresis and no noticeable change in the properties upon repeated cycling (Figure 5b). The uptake of H_2 at 77 K and 800 mmHg is 0.84 wt % (94.27 $cm^3\ g^{-1}$, STP). Moreover, the H_2 isosteric heats of adsorption (Q_{st}) for **4a** calculated from the respective adsorption isotherms at 77 and 87 K, employing the Clausius−Clapeyron equation,[19] are 7.3−7.1 kJ mol^{-1}, depending on the degree of H_2 loading (Figure S5 in the Supporting Information), which is in the usual range of the PMOFs.[20] The approximate value of 7.3 kJ mol^{-1} at zero surface coverage obtained from isotherm studies is close to the corresponding values found for most promising MOFs for hydrogen storage.[21]

Although most adsorption studies on porous materials have been carried out for hydrogen storage purposes in the past few years, there are now increasing investigations aimed at different objectives for other gases, such as CO_2, CH_4, etc.[2d,21b,22] To further check the gas adsorption properties of **4a**, CO_2 and CH_4 adsorption studies have been systematically carried out at 273 K under normal pressure, respectively. All of the adsorption isotherms exhibit typical type I sorption behavior (Figure 5c) and the adsorption capacity of CO_2 is higher than that of CH_4 under the same conditions. At 832 mmHg, **4a** adsorbs CO_2 gas up to 11.21 wt % (57.08 $cm^3\ g^{-1}$, STP), while the adsorb amount of CH_4 at 833 mmHg is 1.02 wt % (14.29 $cm^3\ g^{-1}$, STP), indicating the high selectivity of gas sorption for CO_2 over CH_4. This may mainly be attributed to two factors: (1) The kinetic diameter of the CO_2 molecule (3.3 Å) is smaller than that of the CH_4 molecule (3.8 Å),[23] so that access to the channels in **4a** is easier. (2) The quadrupole moment of CO_2 (-1.4×10^{-39} C m^2) might induce stronger interaction with the porous framework than CH_4.[22e,24]

Luminescent Properties. It is known that many d^{10} metal compounds exhibit luminescent properties.[25] The coordination compounds with the rational selection and design of conjugated organic spacers and metal centers can be efficient for obtaining new luminescence materials.[8e,26,27] To investigate the luminescent properties of complexes **1**−**4**, measurements of the complexes and the H_2ptp ligand were carried out in the solid state at room temperature. As shown in Figure 6, H_2ptp exhibits a blue emission band at 490 nm upon excitation at 360 nm, which could be attributed to intraligand charge transfer (n−π^* or π−π^*). Complexes **1**−**4** present

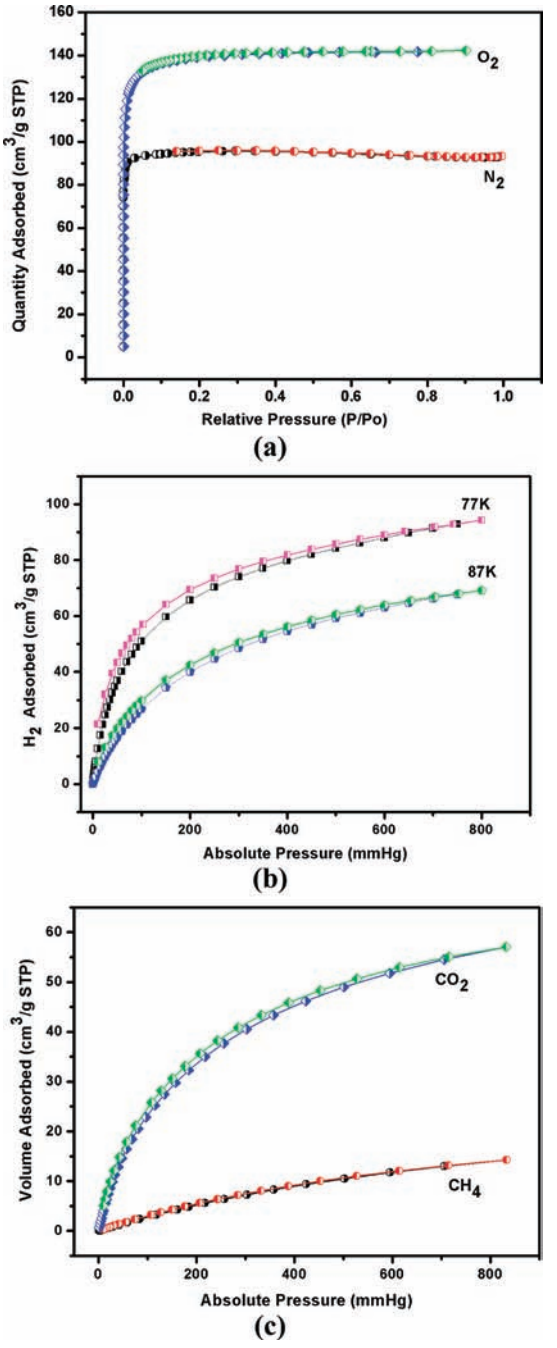

Figure 5. Gas sorption isotherms for **4a**: (a) N_2 and O_2 at 77 K; (b) H_2 at 77 and 87 K; (c) CO_2 and CH_4 at 273 K.

emission bands at 431, 436, 491, and 431 nm upon excitation at 372, 255, 446, and 383 nm, respectively. Compared with emission of the H_2ptp ligand, complexes **1**, **2**, and **4** reveal similar blue shifts of the emission peak and increased luminescent density. These might be attributed to coordination of the ligand ptp^{2-} to Zn^{II} ions, which decreased the nonradiative decay of intraligand excited states. The red shift of the emission spectra of complex **3** suggests an enhancement of π conjugation. All of the emissions of the complexes are tentatively attributed to the intraligand transition (n−π^* and π−π^*) modified by ligation of the ligand to the inactive Zn^{II} ion. To some extent, coordination enhances the "rigidity" of

dx.doi.org/10.1021/ic2015463 |Inorg. Chem. 2011, 50, 10994–11003

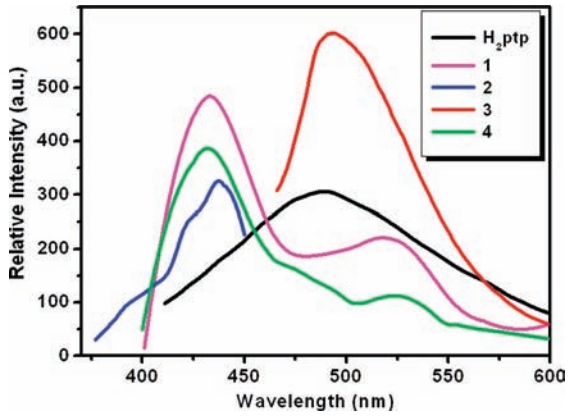

Figure 6. Emission spectra of ligand H_2ptp and complexes **1**−**4** in the solid state at room temperature.

the ligand and thus reduces the loss of energy through a radiationless pathway.[28]

CONCLUSION

A multitopic tetrazolate-based ligand has been used to react with $Zn(NO_3)_2 \cdot 6H_2O$ in solvothermal conditions to give four metal−organic crystalline materials with various structures from a 0D dinuclear molecule to 3D porous frameworks. The various architectures of the four complexes indicated that reaction conditions (temperature and solvent) play important roles in the formation of such coordination structures. It is a remarkable example for obtaining the various frameworks (0D, 1D, 2D, and 3D) by changing the reaction conditions. Moreover, the 3D porous framework with a $(4,12^2)$ topology possesses moderate capability of gas sorption for N_2, H_2, O_2, and CO_2 gases, with high selectivity ratios for O_2 over H_2 at 77 K and CO_2 over CH_4 at 273 K.

ASSOCIATED CONTENT

Supporting Information. X-ray crystallographic files in CIF format for **1**−**4**, selected bond distances and angles for **1**−**4** (Tables S1−S4), dihedral angles between the planes of aromatic heterocycles in ptp^{2-} of **1**−**4** (Table S5), photographs of **1**−**4** (Figure S1), PXRD patterns for **1**−**4** (Figure S2), TGA curve for **4** (Figure S3), the H−K pore-size distribution plot of **4a** (Figure S4), and the isosteric heat of H_2 adsorption for **4a** (Figure S5). This material is available free of charge via the Internet at http://pubs.acs.org.

AUTHOR INFORMATION

Corresponding Author

*E-mail: buxh@nankai.edu.cn. Fax: +86-22-23502458.

ACKNOWLEDGMENT

This work was financially supported by the NNSF of China (Grants 21031002, 20801029, and 51073079) and the NSF of Tianjin, China (Grants 10JCZDJC22100 and 11JCYBJC04100).

REFERENCES

(1) (a) Shimomura, S.; Higuchi, M.; Matsuda, R.; Yoneda, K.; Hijikata, Y.; Kubota, Y.; Mita, Y.; Kim, J.; Takata, M.; Kitagawa, S. *Nat. Chem.* **2010**, *2*, 633. (b) Zeng, Y.-F.; Hu, X.; Liu, F.-C.; Bu, X.-H. *Chem. Soc. Rev.* **2009**, *38*, 469. (c) Sava, D. F.; Kravtsov, V. Ch.; Eckert, J.; Eubank, J. F.; Nouar, F.; Eddaoudi, M. *J. Am. Chem. Soc.* **2009**, *131*, 10394. (d) Cairns, A. J.; Perman, J. A.; Wojtas, L.; Kravtsov, V. Ch.; Alkordi, M. H.; Eddaoudi, M.; Zaworotko, M. J. *J. Am. Chem. Soc.* **2008**, *130*, 1560. (e) Zheng, S.-T.; Zhang, J.; Li, X.-X.; Fang, W.-H.; Yang, G.-Y. *J. Am. Chem. Soc.* **2010**, *132*, 15102. (f) Bu, X.-H.; Tong, M.-L.; Chang, H.-C.; Kitagawa, S.; Batten, S. R. *Angew. Chem., Int. Ed.* **2004**, *43*, 192. (g) Jang, J.-J.; Li, L.; Yang, T.; Kuang, D.-B.; Wang, W.; Su, C.-Y. *Chem. Commun.* **2009**, 2387.

(2) (a) Nouar, F.; Eubank, J. F.; Bousquet, T.; Wojtas, L.; Zaworotko, M. J.; Eddaoudi, M. *J. Am. Chem. Soc.* **2008**, *130*, 1833. (b) Pan, L.; Parker, B.; Huang, X. Y.; Olson, D. H.; Lee, J. Y.; Li, J. *J. Am. Chem. Soc.* **2006**, *128*, 4180. (c) Sun, Y.-Q.; Zhang, J.; Chen, Y.-M.; Yang, G.-Y. *Angew. Chem., Int. Ed.* **2005**, *44*, 5814. (d) Henke, S.; Fischer, R. A. *J. Am. Chem. Soc.* **2011**, *133*, 2064. (e) Fang, Q.-R.; Zhu, G.-S.; Xue, M.; Wang, Z.-P.; Sun, J.-Y.; Qiu, S.-L. *Cryst. Growth Des.* **2008**, *8*, 319.

(3) (a) Chen, S.-S.; Chen, M.; Takamizawa, S.; Chen, M.-S.; Su, Z.; Sun, W.-Y. *Chem. Commun.* **2011**, 752. (b) Mahata, P.; Prabu, M.; Natarajan, S. *Cryst. Growth Des.* **2009**, *9*, 3683. (c) Chaplais, G.; Simon-Masseron, A.; Porcher, F.; Lecomte, C.; Bazer-Bachi, D.; Bats, N.; Patarin, J. *Phys. Chem. Chem. Phys.* **2009**, *11*, 5241.

(4) (a) Li, C.-P.; Du, M. *Chem. Commun.* **2011**, 5958. (b) Chen, S.-C.; Zhang, Z.-H.; Huang, K.-L.; Chen, Q.; He, M.-Y.; Cui, A.-J.; Li, C.; Liu, Q.; Du, M. *Cryst. Growth Des.* **2008**, *8*, 3437. (c) Yin, P.-X.; Zhang, J.; Qin, Y.-Y.; Cheng, J.-K.; Li, Z.-J.; Yao, Y.-G. *CrystEngComm* **2011**, *13*, 3536.

(5) (a) Zhao, Y.-H.; Xu, H.-B.; Fu, Y.-M.; Shao, K.-Z.; Yang, S.-Y.; Su, Z.-M.; Hao, X.-R.; Zhu, D.-X.; Wang, E.-B. *Cryst. Growth Des.* **2008**, *8*, 3566. (b) Su, Z.; Fan, J.; Okamura, T.; Sun, W.-Y.; Ueyama, N. *Cryst. Growth Des.* **2010**, *10*, 3515. (c) Zhang, J.-P.; Chen, X.-M. *Chem. Commun.* **2006**, 1689. (d) Seeber, G.; Cooper, G. J. T.; Newton, G. N.; Rosnes, M. H.; Long, D.-L.; Kariuki, B. M.; Kögerler, P.; Cronin, L. *Chem. Sci.* **2010**, *1*, 62.

(6) (a) Xu, X.-X.; Lu, Y.; Wang, E.-B.; Ma, Y.; Bai, X.-L. *Cryst. Growth Des.* **2006**, *6*, 2029. (b) Shuvaev, K. V.; Abedin, T. S. M.; McClary, C. A.; Dawe, L. N.; Collins, J. L.; Thompson, L. K. *Dalton Trans.* **2009**, 2926.

(7) (a) Hu, T.-L.; Li, J.-R.; Liu, C.-S.; Shi, X.-S.; Zhou, J.-N.; Bu, X.-H.; Ribas, J. *Inorg. Chem.* **2006**, *45*, 162. (b) Lee, Y. J.; Kim, E. Y.; Kim, S. H.; Jang, S. P.; Lee, T. G.; Kim, C.; Kim, S.-J.; Kim, Y. *New J. Chem.* **2011**, *35*, 833.

(8) (a) Dincã, M.; Yu, A. F.; Long, J. R. *J. Am. Chem. Soc.* **2006**, *128*, 8904. (b) Li, J.-R.; Tao, Y.; Yu, Q.; Bu, X.-H. *Chem. Commun.* **2007**, 1527. (c) Li, J.-R.; Tao, Y.; Yu, Q.; Bu, X.-H.; Sakamoto, H.; Kitagawa, S. *Chem.—Eur. J.* **2008**, *14*, 2771. (d) Jiang, C.; Yu, Z.-P.; Jiao, C.; Wang, S.-J.; Li, J.-M.; Wang, Z.-Y.; Cui, Y. *Eur. J. Inorg. Chem.* **2004**, 4669. (e) Jiang, T.; Zhang, X.-M. *Cryst. Growth Des.* **2008**, *8*, 3077.

(9) (a) Dincã, M.; Dailly, A.; Liu, Y.; Brown, C. M.; Neumann, D. A.; Long, J. R. *J. Am. Chem. Soc.* **2006**, *128*, 16876. (b) Ouellette, W.; Prosvirin, A. V.; Whitenack, K.; Dunbar, K. R.; Zubieta, J. *Angew. Chem., Int. Ed.* **2009**, *48*, 2140. (c) Dincã, M.; Dailly, A.; Tsay, C.; Long, J. R. *Inorg. Chem.* **2008**, *47*, 11. (d) Tao, J.; Ma, Z.-J.; Huang, R.-B.; Zheng, L.-S. *Inorg. Chem.* **2004**, *47*, 11.

(10) (a) Popp, F. D. *J. Heterocycl. Chem.* **1974**, *11*, 79. (b) Ried, W.; Aboul-Fetouh, S. *Tetrahedron* **1988**, *44*, 3399. (c) Demko, Z. P.; Sharpless, K. B. *Org. Lett.* **2001**, *3*, 4091. (d) Demko, Z. P.; Sharpless, K. B. *J. Org. Chem.* **2001**, *66*, 7945.

(11) (a) *SAINT Software Reference Manual*; Bruker AXS: Madison, WI, 1998. (b) Sheldrick, G. M. *SHELXTL Version 5.1. Program for Solution and Refinement of Crystal Structures*; University of Göttingen: Göttingen, Germany, 1997. (c) Sheldrick, G. M. *SADABS: Program for Expirical Absorption Correction of Area Detector Data*; University of Göttingen: Göttingen, Germany, 1996.

(12) (a) Chen, X.-M.; Tong, M.-L. *Acc. Chem. Res.* **2007**, *40*, 162. (b) Farha, O. K.; Hupp, J. T. *Acc. Chem. Res.* **2010**, *43*, 1166. (c) Zheng, B.; Dong, H.; Bai, J.; Li, Y.; Li, S.; Scheer, M. *J. Am. Chem. Soc.* **2008**, *130*, 7778. (d) Gándara, F.; Puebla, E. G.; Iglesias, M.; Proserpio, D. M.; Snejko, N.; Monge, M. Á. *Chem. Mater.* **2009**, *21*, 655. (e) Beghidja, A.; Rabu, P.; Rogez, G.; Welter, R. *Chem.—Eur. J.* **2006**, *12*, 7627.

(13) (a) Saalfrank, R. W.; Trummer, S.; Reimann, U.; Chowdhry, M. M.; Hampel, F.; Waldmann, O. *Angew. Chem., Int. Ed.* **2000**, *39*, 3492. (b) Li, Z.; Li, M.; Zhou, X.-P.; Wu, T.; Li, D.; Ng, S. W. *Cryst. Growth Des.* **2007**, *7*, 1992. (c) Rodriguez-Dieguez, A.; Colacio, E. *Chem. Commun.* **2006**, 4140. (d) Ye, Q.; Li, Y.-H.; Song, Y.-M.; Huang, X.-F.; Xiong, R.-G.; Xue, Z.-L. *Inorg. Chem.* **2005**, *44*, 3618. (e) Wang, L.-Z.; Qu, Z.-R.; Zhao, H.; Wang, X.-S.; Xiong, R.-G.; Xue, Z.-L. *Inorg. Chem.* **2003**, *42*, 3969. (f) Xiong, R.-G.; Xue, X.; Zhao, H.; You, X.-Z.; Abrahams, B. F.; Xue, Z.-L. *Angew. Chem., Int. Ed.* **2002**, *41*, 3800.

(14) Hang, T.; Fu, D.-W.; Ye, Q.; Xiong, R.-G. *Cryst. Growth Des.* **2009**, *9*, 2026.

(15) Muppidi, V. K.; Zacharias, P. S.; Pal, S. *Chem. Commun.* **2005**, 2515.

(16) (a) Reger, D. L.; Horger, J. J.; Smith, M. D.; Long, G. J.; Grandjean, F. *Inorg. Chem.* **2011**, *50*, 686. (b) Valencia, L.; Pérez-Lourido, P.; Bastida, R.; Macías, A. *Cryst. Growth Des.* **2008**, *8*, 2080. (c) Kitaura, R.; Seki, K.; Akiyama, G.; Kitagawa, S. *Angew. Chem., Int. Ed.* **2003**, *42*, 428.

(17) Spek, A. L. *PLATON, A Multipurpose Crystallographic Tool*; Utrecht University: Utrecht, The Netherlands, 2006.

(18) (a) Horvath, G.; Kawazoe, K. J. *Chem. Eng. Jpn.* **1983**, *16*, 470. (b) Hou, L.; Lin, Y.-Y.; Chen, X.-M. *Inorg. Chem.* **2008**, *47*, 1346.

(19) Yang, R. T. *Gas Adsorption by Adsorption Processes*; Butterworth: Boston, 1997.

(20) (a) Thomas, K. M. *Dalton Trans.* **2009**, 1487. (b) Murray, L. J.; Dincă, M.; Long, J. R. *Chem. Soc. Rev.* **2009**, *38*, 1294. (c) Ma, S.; Zhou, H.-C. *J. Am. Chem. Soc.* **2006**, *128*, 11734.

(21) (a) Rowsell, J. L. C.; Yaghi, O. M. *J. Am. Chem. Soc.* **2006**, *128*, 1304. (b) Lee, Y.-G.; Moon, H. R.; Cheon, Y. E.; Suh, M. P. *Angew. Chem., Int. Ed.* **2008**, *47*, 7741. (c) Zhao, D.; Yuan, D.; Zhou, H.-C. *Energy Environ. Sci.* **2008**, *1*, 222.

(22) (a) Chen, Z.; Xiang, S.; Arman, H. D.; Mondal, J. U.; Li, P.; Zhao, D.; Chen, B. *Inorg. Chem.* **2011**, *50*, 3442. (b) Mu, B.; Li, F.; Walton, K. S. *Chem. Commun.* **2009**, 2493. (c) Wu, H.; Simmons, J. M.; Liu, Y.; Brown, C. M.; Wang, X. S.; Ma, S.; Peterson, V. K.; Southon, P. D.; Kepert, C. J.; Zhou, H. C.; Yildirim, T.; Zhou, W. *Chem.—Eur. J.* **2010**, *16*, 5205. (d) Cheon, Y. E.; Suh, M. P. *Chem. Commun.* **2009**, 2296. (e) Yoon, J. W.; Jhung, S. H.; Hwang, Y. K.; Humphrey, S. M.; Wood, P. T.; Chang, J. S. *Adv. Mater.* **2007**, *19*, 1830. (f) Zheng, B.; Bai, J.; Duan, J.; Wojtas, L.; Zaworotko, M. J. *J. Am. Chem. Soc.* **2011**, *133*, 748.

(23) Beck, D. W. *Zeolite Molecular Sieve*; John Wiley & Sons: NewYork, 1974.

(24) (a) Lan, A. J.; Li, K. H.; Wu, H. H.; Kong, L. Z.; Nijem, N.; Olson, D. H.; Emge, T. J.; Chabal, Y. J.; Langreth, D. C.; Hong, M. C.; Li, J. *Inorg. Chem.* **2009**, *48*, 7165. (b) Coriani, S.; Halkier, A.; Rizzo, A.; Ruud, K. *Chem. Phys. Lett.* **2000**, *326*, 269. (c) Bae, Y.-S.; Mulfort, K. L.; Frost, H.; Ryan, P.; Punnathanam, S.; Broadbelt, L. J.; Hupp, J. T.; Snurr, R. Q. *Langmuir* **2008**, *24*, 8592.

(25) (a) Aoki, S.; Zulkefeli, M.; Shiro, M.; Kohsako, M.; Takeda, K.; Kimura, E. *J. Am. Chem. Soc.* **2005**, *127*, 9129. (b) Hopkins, T. A.; Meerholz, K.; Shaheen, S.; Anderson, M. L.; Schmidt, A.; Kippelen, B.; Padias, A. B.; Hall, H. K., Jr.; Peyghambarian, N.; Armstrong, N. R. *Chem. Mater.* **1996**, *8*, 344. (c) Santis, G. D.; Fabbrizzi, L.; Licchelli, M.; Poggi, A.; Taglietti, A. *Angew. Chem,. Int. Ed. Engl.* **1996**, *35*, 202. (d) Hu, T.-L.; Zou, R.-Q.; Li, J.-R.; Bu, X.-H. *Dalton Trans.* **2008**, 1302. (e) Chang, Z.; Zhang, A.-S; Hu, T.-L.; Bu, X.-H. *Cryst. Growth Des.* **2009**, *9*, 4840.

(26) (a) Würthner, F.; Sautter, A. *Chem. Commun.* **2000**, 445. (b) Rasika Dias, H. V.; Diyabalanage, H. V. K.; Rawashdeh-Omary, M. A.; Franzman, M. A.; Omary, M. A. *J. Am. Chem. Soc.* **2003**, *125*, 12072. (c) Cariati, E.; Bu, X.; Ford, P. C. *Chem. Mater.* **2000**, *12*, 3385. (d) Ciurtin, D. M.; Pschirer, N. G.; Smith, M. D.; Bunz, U. H. F.; Loye, H.-C. Z. *Chem. Mater.* **2001**, *13*, 2743. (e) Dong, Y.-B.; Wang, H.-Y.; Ma, J.-P.; Shen, D.-Z.; Huang, R.-Q. *Inorg. Chem.* **2005**, *44*, 4679.

(27) (a) Harvey, P. D.; Gray, H. B. *J. Am. Chem. Soc.* **1988**, *110*, 2145. (b) Yam, V. W. W.; Lo, K. K. W. *Chem. Soc. Rev.* **1999**, *28*, 323. (c) Seward, C.; Jia, W.-L.; Wang, R.-Y.; Enright, G. D.; Wang, S. *Angew. Chem., Int. Ed.* **2004**, *43*, 2933. (d) Wu, C.-D.; Ngo, H. L.; Lin, W. *Chem. Commun.* **2004**, 1588. (e) Cui, Y.; Yue, Y.; Qian, G.; Chen, B. *Chem. Rev.* **2011**, DOI: 10.1021/cr200101d.

(28) (a) Zhang, L.-Y.; Zhang, J.-P.; Lin, Y.-Y.; Chen, X.-M. *Cryst. Growth Des.* **2006**, *6*, 1684. (b) Wang, H.-Y.; Gao, S.; Huo, L.-H.; Ng, S. W.; Zhao, J.-G. *Cryst. Growth Des.* **2008**, *8*, 665.